Study of the flow Induced by a Sliding Discharge

R. Sosa, E. Arnaud, G. Artana

Abstract—**In this work, electrical and fluid-dynamics studies have been performed on the flow induced by a sliding discharge (SD) or AC/DC Plasma sheet discharge. The discharge was created with a three-electrode system configuration: one excited with AC and the others with the same DC negative voltage. The SD was activated on a quiescent fluid at atmospheric pressure. The flow field induced by the SD was analysed by means of Pitot probes and Schlieren Image Velocimetry. The induced flows resulted from the electrodes are directed towards the interelectrode space. As a consequence of the mutual interaction of these two flows and of the magnitude of each flow, a plume jet of adjustable direction could be formed. A robust control of the axis direction of the plume could be achieved by modifying the AC voltage value.**

I. INTRODUCTION

Electro-hydrodynamic (EHD) actuators for flow control with aims to aeronautic applications have been receiving special attention in the last years. Through the ionization of flowing air close to the surface of the body, EHD devices produce a modification of the condition of the flow at the wall. As a consequence of the elastic collisions between the migrating charged particles and the neutral species of the gas, the neutrals increase their momentum giving rise to an 'electric wind' that takes place in the close vicinity of the wall. When the number of charged species is high, other mechanisms may also contribute to the electromechanical coupling discharge-airflow like alterations of the physical properties of the gas (density, viscosity, etc) [1]. The EHD devices are technologically attractive because of their simplicity (they have no moving parts) and their very short response time (delays in the establishment of a discharge are theoretically of the order of nanoseconds).

EHD actuators can be classified in three large groups based on the different electrical characteristics of the discharge [2]: dielectric barrier discharge devices (DBD); unipolar coronas discharge based devices (UCD) and plasma sheet discharge devices (PSD).

A large number of studies of flows actuated with DBD have been carried out [3]-[5]. Usual configurations consist on planar parallel electrodes separated by a thin dielectric film, disposed in general in arrangements in the streamwise direction of an aerodynamic surface.

This work was supported by the Argentine government grants UBACYT 0105/I024.

R Sosa is with the University of Buenos Aires, Buenos Aires, Argentina (rsosa@fi.uba.ar).

E. Arnaud is with the University Joseph Fourier and INRIA Rhône-Alpes, France (elise.arnaud@inrialpes.fr)

G. Artana is with the University of Buenos Aires and CONICET, Buenos Aires, Argentina (gartana@fi.uba.ar).

These actuators use periodically excited electrodes, one of them air exposed while the other is encapsulated in a dielectric material. The dielectric barrier interposed between both electrodes plays an important role in the stabilization of the discharge.

UCD are characterized by one active electrode surrounded by an ionization region where free charges are created and low field regions with a large accumulation of space charge where charged particles drift and react in their movement towards the passive electrode [6]-[7].

In PSD an ionized sheet contouring the actuated body is produced with two air exposed electrodes mounted on a dielectric surface. The electrodes excitation can be produced with DC or with a periodic voltage supply that is adjusted to produce an ionization process occupying the whole inter-electrode space. In this region the dielectric surface appears recovered by a thin film of ionized air or plasma sheet. The plasma sheet current includes a DC component and a large number of peaks with frequencies of the order of some kHz [2]. The aerodynamic performances of DC PSD as plasma actuators have been reported in previous works for different flow conditions [8]-[12].

More recently [13], a new sub-group of PSD discharges (AC/DC Plasma sheets) named also sliding discharge devices (SD) has been developed, in order to obtain more stable discharges. This discharge is generated using two electrodes flush mounted on an insulating surface (upper electrodes), and a third electrode placed on the opposite side of the surface facing the upper inter electrode space (lower electrode). A DC negative voltage is applied to one of the two upper electrodes and to the lower electrode, while the other upper electrode is biased with an AC voltage.

The electrical characteristics and aerodynamic performance of these SD devices remain still rather unknown. We propose here to study the flow induced by the SD, when this is applied on quiescent air, in order to optimize their use as a flow control actuator. The aerodynamic effects are evaluated with Pitot measurements close to the air exposed electrodes. Flow visualisations are undertaken by means of tracers not susceptible of charging problems with a Schlieren technique. Quantification of the induced velocity fields is then studied from these images by the use of the Schlieren Image Velocimetry (SIV) [14-15].

II. EXPERIMENTAL SET-UP

The schematic of the experimental set up is shown in figure 1. The electrode arrangement of our experiment consists in two flat aluminium foils air exposed and flush mounted on the dielectric surface (1 and 2). A third one disposed at the opposite side (electrode 3). The electrodes

dimensions are 50 µm thickness, length 400 mm and different widths (5 mm for electrodes 1 and 2 and 30 mm for the electrode 3). The flat plate of support is made of PMMA with a thickness of 4 mm.

A DC power supply (-20 kV, 10 mA) biases electrodes 1 and 3. An AC sine voltage (frequency: f = 9.5 kHz, zero mean value; peak to peak voltage: V_{PP} from 0 to 25 kV) was applied to electrode 2. The AC power supply consists on a HV transformer coil, an audio amplifier of 150 watt and a function generator operating [16].

The electric current flowing in the system, *I(t)*, was measured with a shunt resistance, R = 1 kΩ, connected to an oscilloscope of 1Gs/s (Figure 1). The AC voltage applied to electrode 2, *V(t)*, was measured with a HV probe (1000 × /3.0 pF/100MΩ).

In order to induce almost 2D flows with the SD, the device was placed horizontally in a low speed wind tunnel test section with a section span (450 mm) of the same size than the one of the plate that supported the electrodes.

Two pressure probes (Pitot tubes: P_1 and P_2) of insulating material were placed as is schematically showed in Fig.1. Both Pitots were mounted on the dielectric surface. P_1 was placed 3 mm in front of electrode 1 and P_2 at 3 mm in front of electrode 2. The probes were made of glass tubes of internal diameter: *ID* = 0.97 mm and were connected by means of tygon tubes to a differential pressure transducer. The pressure transducer was one of a variable reluctance type allowing to measure up to 55 Pa with an accuracy of 0.25% full scale. The reference pressure value was measured at the test section but far away from the electrodes.

To complement the induced ionic wind analysis a Schlieren system disposed in a Z configuration was used. It comprised two spherical mirrors of 35 cm in diameter and the light was cut off with two razor blades, thus 2D density gradients could be detected. The parallel light rays traversed the test section of the low speed wind tunnel. Windows of 350mm of optical quality in coincidence with the light beam were mounted on the lateral of the test section to avoid improper light deflections. The images were recorded on a monochromatic digital image camera of 12 bits that enabled fast frame acquisition (i.e. 100 frame/s). In order to improve the image contrast small quantities of Helium were injected vertically from small tubes at some centimetres away from the interelectrode space.

The Schlieren images were analysed with a recently developed method for the estimation of the velocity field: Schlieren Image Velocimetry [14-15].

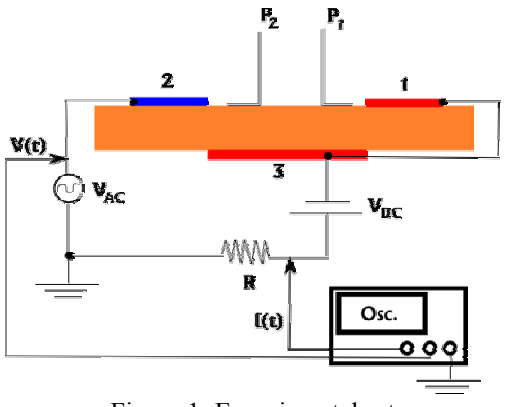

Figure 1: Experimental set-up

III. Experimental Results

Electrical results

The electric current *I(t)* and the AC applied voltage, *V(t)*, of individual signal were recorded. Also by setting the oscilloscope in the average acquisition mode we have acquired the averaged values of these signals over 128 samples:

$$I_m(t) = \frac{1}{128}\sum_1^{128} I(t) \quad (1)$$

$$V_m(t) = \frac{1}{128}\sum_1^{128} V(t) \quad (2)$$

Figure 2 shows typical signals of *I(t)*, $I_m(t)$ and $V_m(t)$, the current, the averaged current and AC voltage respectively.

During the positive part of the AC cycle the potential difference between electrode 2 and 1 permits the ignition of the plasma sheet. As can be observed during this part of the AC cycle the current presents a peak and differs substantially from the capacitive current observed in the negative part of the cycle.

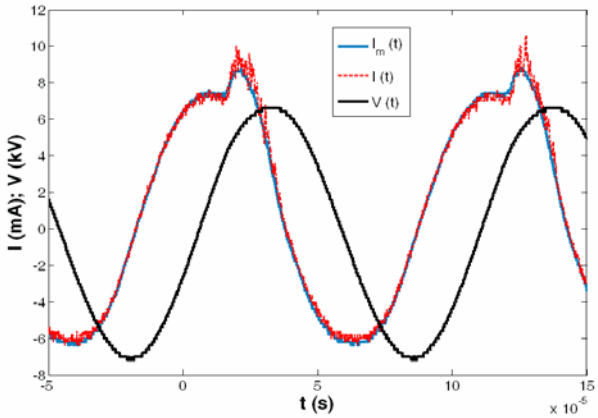

Figure 2: I(t), I_m(t), V_m(t) for V_{DC} = -16 kV,

In order to characterize the electric behavior of SD the active current and the active power were analysed. Strictly these values must be determined using *I(t)* and *V(t)* signals but as only a small error was produced deriving them from the averaged values (I_m and V_m) we have decided to simplify our analysis and just consider the time averaged values. The active current (I_a) and power (P_a) were calculated in consequence as:

$$I_a = \frac{1}{T}\int_0^T I_m(t)dt \quad (3)$$

$$P_a = \frac{1}{T}\int_0^T I_m(t).V_m(t)dt \quad (4)$$

Figure 3 shows the behavior of I_a vs. V_{PP} (peak to peak tension of the AC voltage) for different V_{DC} values. In all these curves it is possible to observe that initially there was an important increase of current with the voltage. This behavior however changed at a given value of V_{pp} (that depended on V_{DC} value) and from this threshold value I_a resulted in an almost linear function of V_{PP} with a more moderate slope. This slope and current values of this "linear

moderate regime" for the different tests were almost independent of the applied DC voltage values. However, the initiation depended on the DC voltage applied to the electrodes. It occurred at lower values of V_{pp} when the negative voltage V_{DC} increased.

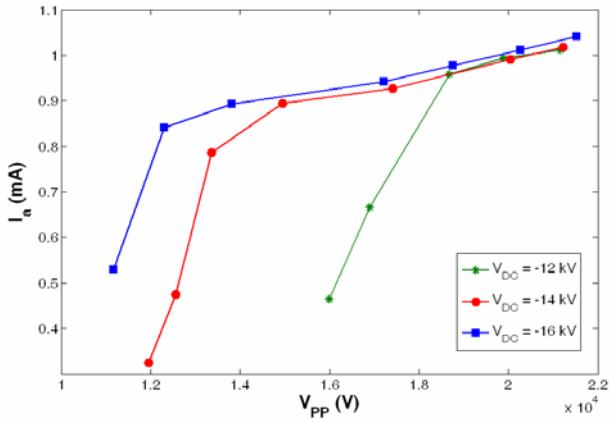

Figure 3: I_a *vs* V_{PP}

In Fig.4 we represent the active power as a function of V_{PP}. For the cases here analysed at values of V_{PP} higher than 1.8 10^4 V, the differences in power consumption for the different V_{DC} values remained almost constant. This behaviour corresponded in fact to the moderate linear regime of I_a vs V_{PP} as for values of $V_{PP} \geq 1.8\ 10^4$ V the I_a values resulted almost independent of the V_{DC} values.

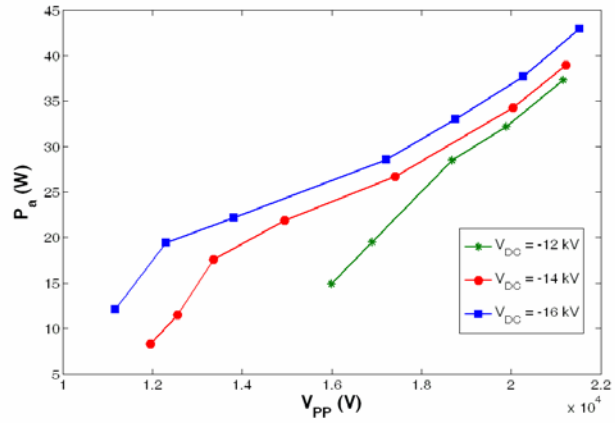

Figure 4: P_a *vs* V_{PP}

Fluid Dynamics results

The induced flow velocities observed with the Pitots P_1 and P_2 (named U_1 and U_2 respectively) can be observed on Fig. 5. These measurements revealed that two distinctive flows directed towards the inter-electrode space were induced from both electrodes. In front of the electrode 2 (acting as anode) the module of the velocity of the induced wind increased almost linearly with the V_{PP} value. This velocity did not show a clear dependency with respect to the V_{DC} values and curves for the different values result almost coincident. On the other hand in face of the electrode 1 (cathode) the induced wind showed an almost constant value or decreased slightly when increasing V_{PP}. Concerning the influence of V_{DC} on these flows we observed that for a given value of V_{pp} the velocity at P_1 resulted higher when V_{DC} value was higher.

In terms of active power the velocity U_2 (figure 6) exhibited a constant slope in correspondence with the linear moderate regime. As can be observed the actuation was more effective to induce flow in this regime and it could not be observed a saturation of velocity with the power. However it should be mentioned that we could not undertake our tests at very large values of power as a consequence of limitations imposed by the maximum power that could be delivered by our experimental setup.

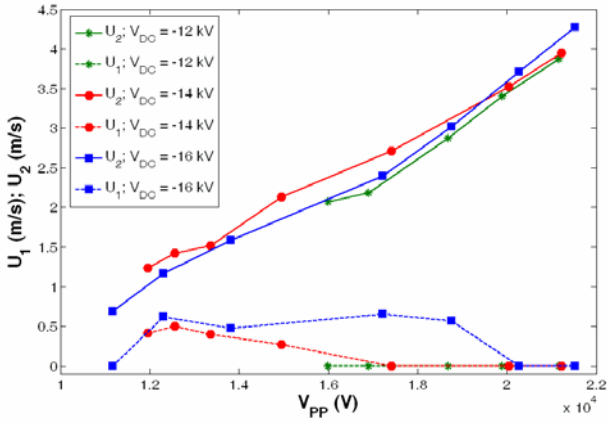

Figure 5: U_1 vs V_{PP} and U_2 vs V_{PP}

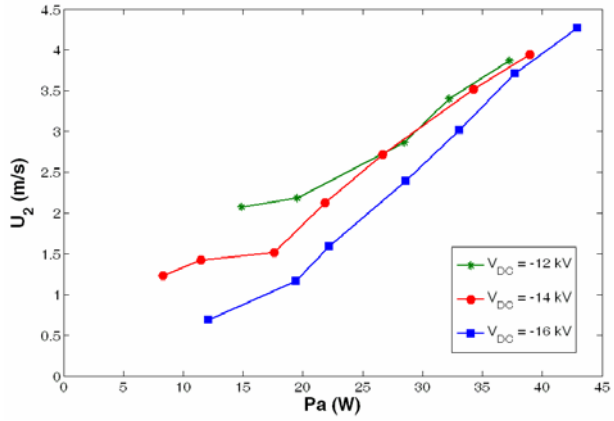

Figure 6: U_2 *vs Pa*

In order to better understand the resulting flow produced by these two opposite induced flows, a set of Schlieren images were processed to obtain the associated velocity fields. Figure 7 shows time averaged velocities fields over 30 instantaneous velocities fields. The electrode arrangement of Fig.7 is consistent with the one of Fig.1

At positions far from the wall the induced flow velocities resulted in general in lower values than the ones observed with P_2. However the discharge-fluid electromechanical coupling is relative high in all cases as the region of neutral gas affected by the SD is relative wide and the action spreads in a relative large region.

Under the conditions Fig. 7a the flows from the electrodes have similar intensities and the interaction between them resulted in a global flow directed to the left of the image.

When the V_{PP} was increased (for the same value of V_{DC} considered) the induced flow from the electrode 2 was increased while the induced flow velocity from the electrode 1 remained almost constant. Under these conditions a global

flow almost perpendicular to the dielectric plate was observed (see Fig.7b).

Finally if the V_{PP} is increased to higher levels (see Fig.7c), the global flow direction was to the right of the image.

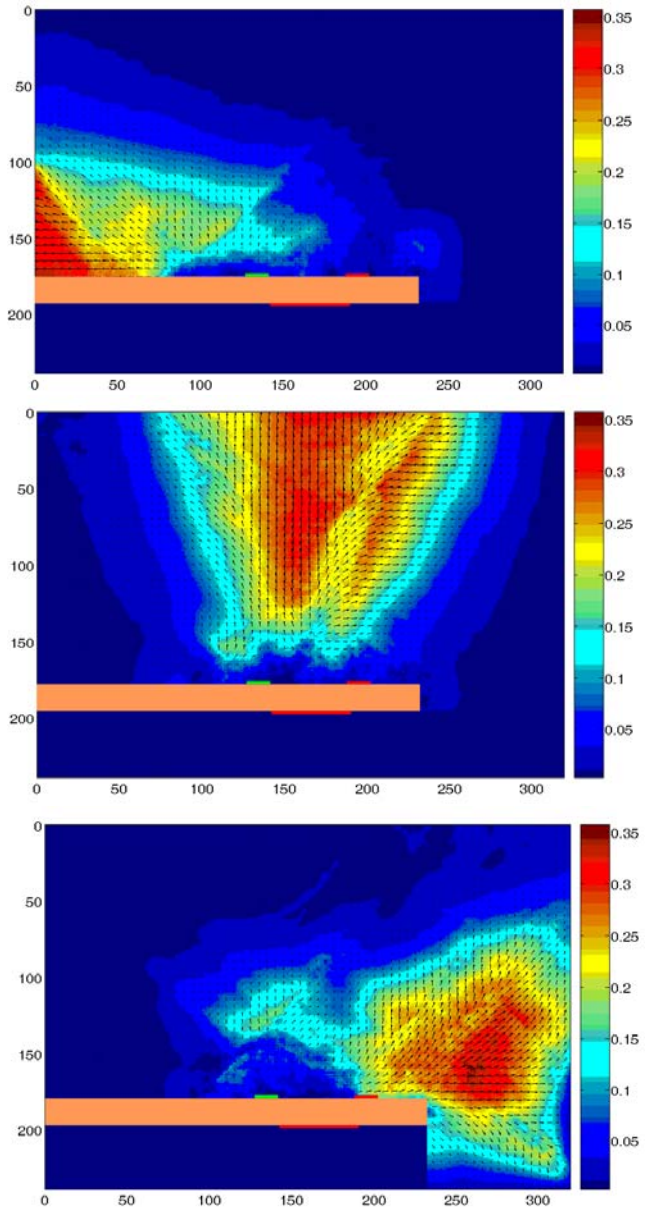

Figure 7: Mean velocity field obtained by (SIV) in m/s
7a. V_{DC} =-18 kV, V_{PP} =12.5 kV, I_a=0.60 mA, P_a=15.84 W
7b. V_{DC} =-18 kV, V_{PP} =18.4 kV, I_a=0.82 mA, P_a=30.46 W
7c. V_{DC} =-18 kV, V_{PP} =21.8 kV, I_a=0.94 mA, P_a=44.31 W
Spatial coordinate units are in px and 1.7 px = 1 mm

IV. FINAL REMARKS

The flow induced by the SD was analysed by means of Pitot on the electrodes proximities and flow field obtained with SIV. The global induced flow result of the interaction between two induced flows parting from the electrodes proximity and directed towards the inter-electrode space. The global induced flow direction resulted strongly dependent on the applied AC voltage. Varying this AC voltage the induced flow direction could span angles almost lying in the range 0-180º.

This work probed that the SD is a promising tool in flow control areas because of their capability to induce a variable direction flow with similar velocities than other plasma actuators with fixed direction of action. The large extension of the ionization region (covering all the inter electrode space) of the SD may produce also substantial alterations of the physical properties of the gas (density, viscosity, etc) in the regions very close to the flow boundaries. Even though this effect could further improve the electomechanical coupling air discharge in different situation this was not explored in this work.

REFERENCES

[1] A Scherbakov et al 2000 Drag reduction by ac streamer corona discharges along a wing-like profile plate AIAA Paper No 2000-2670
[2] R. Sosa, G. Artana, D. Grondona, H. Kelly, A. Márquez and F. Minotti, Discharge characteristics of plasma sheet actuators, Journal of Physics D (2006) in press.
[3] J Roth and D Xin 2006 Optimization of the aerodynamic plasma actuator as an electrohydrodynamic (EHD) electrical device *AIAA* Paper No 2006-1203
[4] T Corke and M Post 2005 Overview of plasma flow control: concepts, optimization, and applications *AIAA* Paper No 2005-563 Reno, Nevada January 2005
[5] S P Wilkinson 2003 Investigation of an oscillating surface plasma for turbulent drag reduction *AIAA* Paper No 2003-1023
[6] G Colver and S El-Khabiry 1999 Modeling of DC corona discharge along an electrically conductive flat plate with gas flow *IEEE Trans. Ind. Appl.* **35** 387–94
[7] C Noger, J S Chang and G Touchard 1997 Active controls of electrohydrodynamically induced secondary flow in corona discharge reactor *Proc. 2nd Int. Symp. on Plasma Technology and Polution Control Bahia, Brazil* pp 136–41
[8] G Artana, J D'Adamo, L Leger, E Moreau and G Touchard 2002 Flow control with electrohydrodynamic actuators *AIAA J.* **40** 1773–9
[9] G Artana, R Sosa, E Moreau and G Touchard 2003 Control of the near wake flow around a circular cylinder with electrohydrodynamic actuators *Exp. Fluids* **36** 580–8
[10] Sosa R and Artana G 2006 Steady control of laminar separation over airfoils with plasma sheet actuators *J. Electrostat.* **64** 604–10
[11] R Sosa, E Moreau, G Touchard and G Artana 2004 Stall control at high angle of attack with periodically excited EHD actuators AIAA Oregon *AIAA* Paper No 2004-2738
[12] R Sosa, G Artana, E Moreau, G Touchard, Stall control at high angle of attack with plasma sheet actuators, In press in *Experiments in fluids*
[13] C. Louste, G. Artana, E. Moreau, G. Touchard "Sliding discharge in air at atmospheric pressure: electrical properties," *Journal of Electrostatic*, Vol. 63, 2005, pp. 615-620.
[14] R Sosa., E Arnaud., E Memin., G Artana., Schlieren Image Velocimetry applied to EHD flows, International Simposium on Electrohydrodonamics (ISEHD), 4-6 december, Buenos Aires, Argentina
[15] E. Arnaud, E. Memin, R. Sosa, and G. Artana A Fluid Motion Estimator for Schlieren Image Velocimetry, Lecture Notes in Computer Science, 3951 / 2006 , pp. 198 - 210
[16] Manish Yadav 2005 Pitot tube and wind tunnel studies of the flow induced by one atmosphere uniform glow discharge (oaugdp®) plasma actuators using a conventional and an economical high voltage power supply MS Thesis Department of Physics, University of Tennessee